J Mol Model (2014) 20:2412
DOI 10.1007/s00894-014-2412-4

ORIGINAL PAPER

# On the chemical behavior of $C_{60}$ hosting $H_2O$ and other isoelectronic neutral molecules

**Annia Galano · Adriana Pérez-González · Lourdes del Olmo · Misaela Francisco-Marquez · Jorge Rafael León-Carmona**

Received: 10 February 2014 / Accepted: 30 July 2014 / Published online: 14 August 2014


**Abstract** The density functional theory (DFT) was used to investigate the chemical behavior of $C_{60}$ hosting neutral guest molecules (NGM). The deformed atoms in molecules (DAM) allowed identifying the regions of electron density depletion and accumulation. The studied NGM are $CH_4$, $NH_3$, $H_2O$, and HF. Based on dipole moment and polarizabilities analyses it is predicted that the NGM@$C_{60}$ should be more soluble in polar solvents than $C_{60}$. The deformations on the surface electron density of the fullerenes explain this finding, which might be relevant for further applications of these systems. It was found that the intrinsic reactivity of studied NGM@$C_{60}$ is only moderately higher than that of $C_{60}$. This trend is supported by the global reactivity indexes and the frontier orbitals analyses. The free radical scavenging activity of the studied systems, via single electron transfer, was found to be strongly dependent on the chemical nature of the reacting free radical. The presence of the studied NGM inside the $C_{60}$ influences only to some extent the reactivity of $C_{60}$ toward free radicals. The distortion of the electron density on the $C_{60}$ cage, caused by the NGM, is directly related to the electron withdrawing capacity of the later.

**Keywords** Deformed atoms in molecules · Free radicals · Fullerene · Rate constants · Reactivity indexes · Solubility

This paper belongs to Topical Collection QUITEL 2013

**Electronic supplementary material** The online version of this article (doi:10.1007/s00894-014-2412-4) contains supplementary material, which is available to authorized users.

A. Galano (✉) · A. Pérez-González · J. R. León-Carmona
Departamento de Química, Universidad Autónoma Metropolitana-Iztapalapa, San Rafael Atlixco 186, Col. Vicentina. Iztapalapa., C. P. 09340 México, D. F., Mexico
e-mail: agalano@prodigy.net.mx

L. del Olmo
Departamento de Química Física Aplicada, Facultad de Ciencias, Universidad Autónoma de Madrid, 28049 Madrid, Spain

M. Francisco-Marquez
Instituto Politécnico Nacional-UPIICSA, Té 950, Col. Granjas México, C.P. 08400 México, D. F., Mexico

J. R. León-Carmona
Instituto de Investigaciones en Materiales, Universidad Nacional Autónoma de México, Circuito Ext. s/n, Ciudad Universitaria, Coyoacán, P. O. Box 70-360, 04510 México, D. F., Mexico

## Introduction

Since the discovery of $C_{60}$, modified fullerenes have become the subject of many experimental and theoretical investigations due to their potential on tuning the chemical and physical properties of this molecule. One of these modifications consists of incorporating atoms, ions, small molecules, or clusters inside the carbon cage [1–10], i.e., yielding endohedral fullerenes. Most of the methods used for synthesizing these nanosystems involve harsh conditions [11, 12], which makes them unsuitable for producing fullerenes hosting neutral guest molecules (NGM). However, this can be achieved using a recently developed synthetic strategy known as molecular surgery [11, 13–15]. The synthesis of $H_2O$@$C_{60}$ is a successful example of such a procedure [11].

This particular molecular system has attracted great attention due to its amazing features. For example, it presents a hydrophobic cavity containing a single polar molecule [12]. This causes that while $C_{60}$ itself does not have a dipole moment, $H_2O$@$C_{60}$ is a polar molecule [11]. The encapsulated water molecule cannot undergo conventional H bonding [16], which may be very important for understanding the properties of $H_2O$ when it is not connected this way with its neighbors [12]. Accordingly, several studies, both

experimental [17–19] and theoretical [12, 20–24], have been devoted to study fullerenes containing water molecules.

To our best knowledge $H_2O@C_{60}$ is the only endohedral fullerene containing a NGM that has been synthesized so far. However, theoretical studies have been performed on other $NGM@C_n$ systems and some of their properties have been predicted. Rehaman et al. reported the structure and infrared (IR) spectra of $CH_4@C_{84}$ and $CH_4@C_{60}$ [25]. Ren et al. proposed the structure, formation energy, energy gap between the highest occupied molecular orbital (HOMO) and the lowest unoccupied molecular orbital (LUMO), electron affinity (*EA*), ionization potential (*IP*), IR active modes, and harmonic vibrational frequencies of $C_4H_4@C_{60}$ [26] and $C_4H_4@C_{70}$ [27]. Wang et al. calculated the $^1H$ NMR chemical shifts of fullerene compounds hosting $H_2$, $H_2O$, and $NH_3$ [28]. Peng et al. estimated the structure, stability, and electronic properties of $GeH_4@C_{60}$ [29]. Medrek et al. modeled the structures and energies of the inclusion complexes of $C_{60}$ with $H_2O$, $NH_3$, $H_2$, $2H_2$, $3H_2$, $4H_2$, $O_2$, and $O_3$ [30]. Accordingly it can be stated that theoretical studies are contributing to an anticipated knowledge of this particular kind of endohedral fullerenes. Due to the spectacular growth of computational power in the last decades, currently it is possible to obtain reliable data from calculations at a reasonable computational cost for these systems. Moreover, taking advantage of computational studies to address the investigation of $NGM@C_n$ systems seems to be a very appealing option.

In addition, since the door to the synthesis of fullerenes hosting NGM was opened only a few years ago, these nanoobjects have been considerably less studied than some of their relatives such as endohedral metallofullerenes. An important issue that naturally arises when any molecular system is structurally modified is the role of such modification on the chemical properties. Therefore, studies allowing comparisons between the endohedral fullerenes and the isolated host and guest molecules are very important to quantify the influence of the encapsulation on the properties of the combined system. For example the importance of works investigating the extent of the effects of the internal $H_2O$ molecule on the reactivity of $H_2O@C_{60}$ has been recently pointed out [16].

Accordingly it is the main goal of the present work to investigate some properties of $C_{60}$ hosting $H_2O$ and other isoelectronic NMG ($CH_4$, $NH_3$, and HF), most of them related to chemical reactivity. With that goal in mind we report here binding energies per C atom, dipole moments, polarizabilities, electron densities, HOMO and LUMO energies, HOMO-LUMO gaps, and reactivity indexes. In addition, several studies on the ability of fullerenes to easily react with free radicals have also been reported [31–35]. This is a very desirable property due to the damaging effects of free radicals, with both environmental and health implications. Accordingly the role of the guest molecule on the potential free radical scavenging activity of the studied $NGM@C_{60}$ systems has also been investigated.

## Computational details

All the electronic calculations have been carried out with the package of programs Gaussian 09 [36]. Full geometry optimizations and frequency calculations were carried out using the density functional BPW91 and the valence double-zeta D95V [37] basis set. This functional combines the Becke's 1988 exchange functional [38], which includes the Slater exchange along with corrections involving the gradient of the density, with Perdew and Wang's 1991 gradient-corrected correlation functional [39–42]. The BPW91 functional was chosen after testing the quality of the results obtained with different methods vs. some available experimental data (for details see the subsection Choosing the calculation method, in the Results and discussion section). The energies were improved by single point calculations at the BPW91/6-311+G(d) level of theory, which includes a larger (triple zeta) basis set with polarization and diffuse functions. This dual level strategy is commonly employed for large systems, and implies assuming that geometries are close enough at both levels of theory. This is usually the case, since geometries are not particularly sensitive to changes in basis sets, provided that the low level basis set is not too small. The located stationary points were confirmed to correspond to local minima by the absence of imaginary frequencies. Thermodynamic corrections at 298 K were included in the calculation of relative energies.

For the calculations related to the free radical scavenging activity of the studied systems, solvent effects were included, a posteriori, using the SMD continuum model [43] with benzene and water as solvents to mimic polar and non-polar environments. The electron densities on the different molecular structures were obtained from the deformed atoms in molecules (DAM) approach, using the DAMQT package of programs [44]. The DAM allows mapping the molecular regions of electron density depletion and accumulation, and this information has been used to rationalize the trends in properties found for the systems of interest.

## Results and discussion

### Choosing the calculation method

The performance of different calculation methods was tested by comparisons with available experimental data. The data set includes the vertical ionization energy (*IE*), the vertical electron affinity (*EA*) and the HOMO-LUMO gap (*HLg*) of $C_{60}$. The tested methods are: BPW91, B3LYP, cam-B3LYP, PBE, TPSS, TPSSh, M05-2X, B97D, and BHandHLYP. In addition calculations performed using MP2 at the BHandHLYP geometries were also included. All of them were used in conjunction with the D95V basis set.

It was found that the smallest mean unsigned errors (MUE) for IE and EA correspond to the calculations performed with the BPW91 and the B3LYP functional (Table 1). The MUE in these two cases were lower than 0.1 eV. For the *HLg*, on the other hand the calculations that produce the values closest to the experimental one are those performed with the BPW91, TPSS, and B97D (Table 2). For all of them the deviation from the experimental value is lower than 0.2 eV. For the polarizability of $C_{60}$, the smallest deviations (lower than 1 Å$^3$) were found for BPW91, PBE, TPSS, and TPSSh.

Accordingly, BPW91 is the only method, among the tested functionals, best reproducing all the experimental data (ionization energies, HOMO-LUMO gap, and polarizability). Based on these results this functional was chosen to calculate these and all the other properties presented here for $C_{60}$ and its studied NGM@$C_{60}$ derivatives.

## Binding energies per C atom (eV)

Changes in the binding energy per C atom ($BE_{/C\ atom}$) are important for possible modifications on the C network of fullerenes. It is dominated by strong localized covalent bonding through sp$^2$ carbon orbitals and by delocalized π orbitals. Accordingly, we have investigated whether the inclusion of the studied NGM inside the $C_{60}$ cage can influence its $BE_{/Catom}$.

The binding energy per C atom has been calculated with respect to dissociation into elements, as:

$$BE_{/C\,atom} = \frac{E_{C60} - 60E_C}{60} \quad (1)$$

**Table 1** Vertical ionization energies (*IE*, eV), vertical electron affinities (*EA*, eV), signed errors (*SE*, eV) with respect to the experimental values, and mean unsigned error (*MUE*, eV), arising from different methods of calculation

| | *IE* | *SE* | *EA* | *SE* | *MUE* |
|---|---|---|---|---|---|
| BPW91 | 7.46 | −0.14 | 2.76 | 0.04 | 0.09 |
| B3LYP | 7.63 | 0.03 | 2.64 | −0.08 | 0.06 |
| cam-B3LYP | 8.01 | 0.41 | 2.42 | −0.30 | 0.36 |
| PBE | 7.45 | −0.15 | 2.81 | 0.09 | 0.12 |
| TPSS | 7.36 | −0.24 | 2.69 | −0.03 | 0.13 |
| TPSSh | 7.49 | −0.11 | 2.64 | −0.08 | 0.10 |
| M05-2X | 8.22 | 0.62 | 2.64 | −0.08 | 0.35 |
| B97D | 7.32 | −0.28 | 2.69 | −0.03 | 0.16 |
| BHandHLYP | 7.80 | 0.20 | 2.27 | −0.45 | 0.32 |
| MP2/BHandHLYP | 7.42 | −0.18 | 2.89 | 0.17 | 0.18 |
| Exp. | 7.6 [45] | | 2.72 [46] | | |

**Table 2** HOMO-LUMO gaps (*HLg*, eV), polarizabilities (α, Å$^3$), and signed errors (*SE*, eV) with respect to the experimental values, from different methods of calculation

| | *HLg*[a] | *SE* | α | *SE* |
|---|---|---|---|---|
| BPW91 | 1.63 | −0.17 | 77.26 | 0.86 |
| B3LYP | 2.69 | 0.89 | 75.03 | −1.37 |
| cam-B3LYP | 4.84 | 3.04 | 72.10 | −4.30 |
| PBE | 1.62 | −0.18 | 77.10 | 0.70 |
| TPSS | 1.68 | −0.12 | 76.70 | 0.30 |
| TPSSh | 2.21 | 0.41 | 75.48 | −0.92 |
| M05-2X | 4.56 | 2.76 | 72.74 | −3.66 |
| B97D | 1.63 | −0.17 | 77.40 | 1.00 |
| BHandHLYP | 4.36 | 2.56 | 71.86 | −4.54 |
| MP2/BHandHLYP | 7.09 | 5.29 | | |
| Exp. | 1.8 [47] | | 76.4 [48] | |

[a] $HLg = E_{LUMO} - E_{HOMO}$

$$BE_{/C\,atom} = \frac{E_{NGM@C60} - 60E_C - E_{NGM}}{60} \quad (2)$$

where $E_C$ represents the energy of each C atom.

All the binding energies were found to be negative (Table 3), supporting the stability of the studied NGM@$C_{60}$ derivatives. The influence of the guest on the $BE_{/Catom}$ of $C_{60}$ was found to be negligible, smaller than 0.03 kcal mol$^{-1}$, in all the studied cases. This suggests that the mechanical properties of $C_{60}$ should not be affected by the inclusion of the studied NGM inside the cage.

## Dipole moments and polarizabilities

Dipole moments (μ) play an important role in the solubility of molecular systems, as well as on their possible interactions with neighbor species, for which polarizabilities (α) are also important. Therefore, both properties have been estimated for the systems under study.

Our results show that the inclusion of the studied guest molecules inside the non-polar $C_{60}$ carbon cage, causes the complex systems to have a permanent dipole moment. It is

**Table 3** Binding energies per C atom in kcal mol$^{-1}$, calculated at the BPW91/6-311+G(d)//BPW91/D95V level of theory

| | $\Delta E^a$ | $\Delta H$ | $\Delta G$ |
|---|---|---|---|
| $C_{60}$ | −7.03 | −7.08 | −6.65 |
| $CH_4$@$C_{60}$ | −7.02 | −7.07 | −6.63 |
| $NH_3$@$C_{60}$ | −7.02 | −7.08 | −6.64 |
| $H_2O$@$C_{60}$ | −7.03 | −7.08 | −6.65 |
| HF@$C_{60}$ | −7.03 | −7.08 | −6.65 |

[a] Including zero point energy (ZPE) corrections

interesting that this is the case even when $CH_4$ is the guest molecule, despite the fact that both $C_{60}$ and $CH_4$ have $\mu'=0$ when they are isolated. Of course for this particular case the resulting dipole moment in the complex system is very small. On the other hand the presence of the studied polar NGM ($NH_3$, $H_2O$, and HF) lead to rather significant dipole moments for the NGM@$C_{60}$ systems. As intuitively expected, those with the largest $\mu$ are the ones with the most polar guest molecule ($H_2O$ and HF). It should be noted, however, that taking into account that the calculated dipole moments of $H_2O$ and HF are overestimated by about 0.6 and 0.4 D, respectively, the values reported here for the NGM@$C_{60}$ systems can be taken as upper limits.

In all the studied cases that involve $C_{60}$ hosting polar NGM, the dipole moment of the complex system was found to be lower than that of the corresponding isolated NGM (Table 4). This is in agreement with previous calculations for $H_2O$@$C_{60}$ [20, 21].

The finding that the NGM@$C_{60}$ systems with NMG=$NH_3$, $H_2O$, and HF have a permanent dipole moment, indicates that the solubility of such systems in polar solvents should be higher than that of the empty $C_{60}$. In addition, their interactions with polar molecules in their surrounding should be stronger, also compared to $C_{60}$. The NGM@$C_{60}$ systems are predicted to be more polarizable than the empty cage (Table 4). The system with the highest polarizability was found to be $CH_4$@$C_{60}$. This increased polarizability might also contribute to a higher solubility in polar solvents.

To provide further insights on the above described behavior, we have analyzed the DAM of the studied molecules (Fig. 1). The trend found for dipole moments can be rationalized based on the regions of density concentration and depletion on the carbon cages (view 1, Fig. 1). The depletion zones were found to be aligned with the H atoms in the NGM. Thus, the largest dipole moment corresponds to HF@$C_{60}$, which presents the most localized depletion (blue in Fig. 1), essentially placed in one single region on the cage surface. In the series HF@$C_{60}$, $H_2O$@$C_{60}$, $NH_3$@$C_{60}$, $CH_4$@$C_{60}$, $C_{60}$, the largest depletion regions increase in number, and are distributed in a more homogeneous way. Therefore, going from HF@$C_{60}$ to $CH_4$@$C_{60}$ the dipole moment decreases. It becomes zero for $C_{60}$ due to the perfect symmetric distribution of density depletion and concentration regions on the surface of the empty fullerene. The $CH_4$@$C_{60}$ molecule is an interesting case that comprises a non-polar guest molecule inside a non-polar cage, however leading to a system with a small dipole moment. This can be explained by the finding that the depletion zones do not accurately cancel out, because their sizes and shapes are not precisely the same and their position are not exactly opposed.

Regarding the polarizabilities, a direct relationship was found with the electron density concentration on the surface of the fullerene cages (view 2, Fig. 1). Probably the most unexpected behavior corresponds to $C_{60}$, which presents the lowest polarizability within the studied set of systems. This can be explained by the fact that this particular structure

**Table 4** Dipole moments ($\mu'$), and mean polarizabilities ($\alpha$), calculated at the BPW91/6-311+G(d)//BPW91/D95V level of theory

| | $\mu'$ (D)[a] | $\alpha$ (Å$^3$) | | $\mu'$ (D) | $\alpha$ (Å$^3$) |
|---|---|---|---|---|---|
| $C_{60}$ | 0.000 | 77.26 | | | |
| $CH_4$@$C_{60}$ | 0.002 | 77.80 | $CH_4$ | 0.000 | 1.77 |
| $NH_3$@$C_{60}$ | 0.271 | 77.57 | $NH_3$ | 1.246 | 1.36 |
| $H_2O$@$C_{60}$ | 0.405 | 77.44 | $H_2O$ | 2.450 | 0.23 |
| HF@$C_{60}$ | 0.436 | 77.36 | HF | 2.236 | 0.11 |

[a] The $\mu'$ symbol is used to differentiate from the chemical potential ($\mu$)

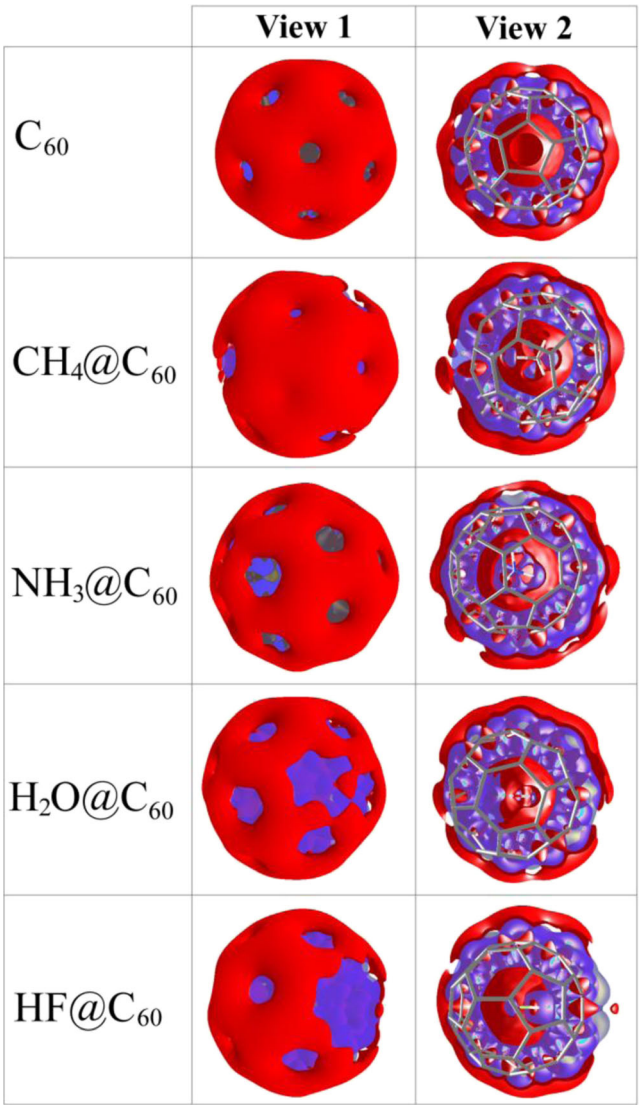


**Fig. 1** Deformed atoms in molecules (DAM) for the studied fullerenes. Regions of electron density depletion and concentration are presented in blue and red, respectively. View 1 shows the complete perspective and view 2 corresponds to the cross-sections. Contour values: ±0.001

presents the largest electron density concentration within the cavity, causing a reduced density on the surface, compared to the other systems. For the rest of the series the order in polarizability is in line with that of the isolated NGM. This can also be explained by the DAM which shows that as the regions of density depletion on the C cage surface increases the polarizability lowers.

## HOMO and LUMO energies

It is currently well known that the frontier molecular orbitals (HOMO and LUMO) play an important role in chemical reactivity [49, 50]. The HOMO-LUMO gap has been used as a measure of the kinetic stability for π conjugated systems in general, and for fullerenes in particular [51–53]. The energies of these orbitals have been associated with the chemical reactivity of fullerenes [51] since adding electrons to a low lying LUMO, or removing electrons from a high lying HOMO, are energetically favorable processes. Accordingly, we have analyzed the HOMO and LUMO energies, as well as the energy gap between them for the studied NGM@$C_{60}$ systems.

Our results (Table 5) indicate that the HOMO-LUMO gap is reduced when $C_{60}$ is hosting the isoelectronic NGM studied in this work, $CH_4$, $NH_3$, $H_2O$, and HF. This reduction was found to be larger for $NH_3$, $H_2O$, and HF than for $CH_4$, which suggests that the reactivity of the NGM@$C_{60}$ system increased with the polarity of the guest. In addition the inclusion of the NMGs in the cavity of $C_{60}$ increases the HOMO energy, indicating that the ability of endofullerenes to donate electrons should be higher than that of the empty $C_{60}$. For the opposite process, the systems with $C_{60}$ hosting NMG are not expected to be as good as the empty cage for accepting electrons since the lowest energy of the LUMO corresponds to $C_{60}$. It should be noted that the differences for HOMO and LUMO energies, as well as for the *HLg*, between $C_{60}$ and the studied NGM@$C_{60}$ systems are very small; thus these criteria suggest only slight changes in reactivity due to the presence of the NGM.

**Table 5** Energies of the highest occupied molecular orbital (HOMO) and the lowest unoccupied molecular orbital (LUMO), and HOMO-LUMO energy gap (*HLg*); calculated at the BPW91/6-311+G(d)//BPW91/D95V level of theory

| | $E_{HOMO}$ (eV) | $E_{LUMO}$ (eV) | *HLg*[a] (eV) |
|---|---|---|---|
| $C_{60}$ | −5.908 | −4.279 | 1.629 |
| $CH_4$@$C_{60}$ | −5.893 | −4.273 | 1.620 |
| $NH_3$@$C_{60}$ | −5.878 | −4.276 | 1.602 |
| $H_2O$@$C_{60}$ | −5.867 | −4.266 | 1.601 |
| HF@$C_{60}$ | −5.882 | −4.281 | 1.601 |

[a] $HLg = E_{LUMO} - E_{HOMO}$

## Global reactivity indexes

Chemical reactivity descriptors (also known as reactivity indexes) naturally arise from the DFT formalism and provide valuable information on the intrinsic reactivity of molecular systems. Those analyzed in this work are hardness ($\eta$), chemical potential ($\mu$), electronegativity ($\chi$), electrophilicity ($\omega$), electroaccepting power ($\varpi^{+}$), and electrodonating power ($\varpi^{-}$).

Vertical ionization energies (*IE*) and vertical electron affinities (*EA*) used to estimate the above described reactivity indexes were calculated as:

$$IE = E_{N-1}(g_N) - E_N(g_N) \tag{3}$$

$$EA = E_N(g_N) - E_{N+1}(g_N) \tag{4}$$

where $E_N(g_N)$ is the energy of the *N*-electron system calculated at the geometry $g_N$ and $E_{N-1}(g_N)$ and $E_{N+1}(g_N)$ are the energies of the $(N-1)$ and $(N+1)$ electron systems, calculated also at the $g_N$ geometry.

First *IE* and *EA* themselves can also be used as global reactivity indexes that allow quantifying the tendency of a system to donate or accept, respectively, one electron. The values reported in Table 6 indicate that, compared to $C_{60}$, the energy required for the first ionization of the NGM@$C_{60}$ is lower when NGM=$CH_4$ and $H_2O$ (with the lowest value corresponding to $CH_4$@$C_{60}$); the same when NGM=HF; and higher when NGM=$NH_3$. This means that one possible strategy for improving the ability of $C_{60}$ to donate one electron might be including one molecule of $H_2O$ or $CH_4$ inside the cage, and that the latter would be a better choice. For the *EA*, on the other hand, the encapsulation of all the studied NGM within the carbon cage is predicted to increase the ability of $C_{60}$ to accept one extra electron. However, the largest effect arises when $NH_3$ is the guest molecule. These findings seem to be relevant for possible electron transfer reactions from and toward fullerenes. The implications for the potential free radical scavenging activity of these nano-systems will be discussed in the following section.

The global hardness$\eta$, defined by Parr and Pearson [54] as the second derivative of the electronic energy of the system with respect to the number of electrons at a constant external potential:

$$\eta = \frac{1}{2}\left(\frac{\partial^2 E}{\partial N^2}\right)_{\nu(r)} \tag{5}$$

has been calculated in a finite-difference approximation, with the assumption that the energy varies quadratically with the

**Table 6** Vertical ionization energies (*IE*), electron affinities (*EA*), hardness ($\eta$), electronegativities ($\chi$), electrophilicities ($\omega$), electrodonating powers ($\varpi^-$), and electroaccepting powers ($\varpi^+$), all in eV; calculated at the BPW91/6-311+G(d)//BPW91/D95V level of theory

| | *IE* | *EA* | $\eta$ | $\chi$ | $\omega$ | $\varpi^-$ | $\varpi^+$ |
|---|---|---|---|---|---|---|---|
| $C_{60}$ | 7.457 | 2.762 | 2.347 | 5.109 | 5.561 | 8.409 | 3.300 |
| $CH_4@C_{60}$ | 7.425 | 2.781 | 2.322 | 5.103 | 5.608 | 8.449 | 3.346 |
| $NH_3@C_{60}$ | 7.460 | 2.799 | 2.331 | 5.129 | 5.644 | 8.500 | 3.371 |
| $H_2O@C_{60}$ | 7.446 | 2.789 | 2.329 | 5.118 | 5.623 | 8.473 | 3.356 |
| $HF@C_{60}$ | 7.457 | 2.772 | 2.343 | 5.114 | 5.582 | 8.432 | 3.318 |

number of electrons, as:

$$\eta = \frac{IE - EA}{2} \tag{6}$$

where *IE* and *EA* stand for vertical ionization energy and vertical electron affinity, respectively.

While the non-chemical meaning of the word "hardness" is resistance to deformation or change, the chemical hardness measures resistance to change in electron number or in the shape of the electron cloud. Therefore, the chemical hardness generally measures the energy required for a chemical system to store charge. The hardness of all the studied NGM@$C_{60}$ systems (Table 6) was found to be lower than that of empty $C_{60}$, indicating that the ability for charge storage is increased when this fullerene is hosting NGM. These results might have implications for the potential use of these systems as electronic devices.

The chemical potential ($\mu$) is defined, within the frame of the density-functional theory as the partial derivative of the system's energy ($E$) with respect to the number of electrons ($N$) at a fixed external potential $\nu(r)$:

$$\mu = \left(\frac{\partial E}{\partial N}\right)_{\nu(r)} \tag{7}$$

It measures the escaping tendency from an electronic cloud. It is constant, through all the space, for the ground state of atoms, molecules or solids. The chemical potential is the negative of the electronegativity ($\chi$) concept of Pauling and Mulliken [55], which according to Mulliken's formula [56] can be calculated as:

$$\chi = \frac{IE + EA}{2} = -\mu \tag{8}$$

Differences in $\chi$ drive electron transfer. Electrons tend to flow from a region of low electronegativity to a region of high electronegativity and the number of electrons that flow is linearly proportional to the $\chi$ differences, while the concurrent energy stabilization is proportional to its square. Electronegativities equalize in polyatomic systems, all becoming equal to the electronegativity of the final molecule (Sanderson's principle). As the results reported in Table 6 show, the inclusion of $NH_3$, $H_2O$, and HF inside $C_{60}$ increases, while the inclusion of $CH_4$ slightly decreases, the electronegativity of the system, compared to that of the empty cage. Accordingly it can be stated that the presence of a polar NGM inside the cage would promote the electron flow toward the fullerene.

Electrophilicity is another important descriptor since its value would determine the chemical behavior of the reacting species, i.e., in a chemical reaction involving two molecules the one with the higher electrophilicity will act as the electrophile, while the other (with lower electrophilicity) will behave as a nucleophile [57]. In this work $\omega$ has been calculated as:

$$\omega = \frac{(IE + EA)^2}{8(IE - EA)} \tag{9}$$

as proposed by Parr et al. [58] for the ground-state parabola model. It was found (Table 6) that the electrophilicity of $C_{60}$ is increased when hosting all the studied NGM. This indicates that the electrophilic character of the NGM@$C_{60}$ systems is higher than that of the empty fullerene.

The electrodonating power ($\varpi^-$) and the electroaccepting power ($\varpi^+$) indexes have been recently proposed by Gázquez et al. [59]. They are ideal for describing the propensity of a given chemical species to donate or accept fractional amounts of charge. They are expected to show a similar behavior to that of the first ionization potential and the electron affinity, respectively. However, while *IE* and *EA* measure the capability of a chemical system to donate or accept one electron, $\varpi^+$ and $\varpi^-$ measure the capability of a chemical system to donate or to accept a small fractional amount of charge [60]. These indexes are calculated according to:

$$\varpi^+ = \frac{(IE + 3EA)^2}{16(IE - EA)} \tag{10}$$

and

$$\varpi^- = \frac{(3IE + EA)^2}{16(IE - EA)} \tag{11}$$

It was found that for the electroaccepting power ($\varpi^+$) the trends are the same as those already discussed for *EA* (Table 6), i.e., the ability of accepting (fractional) charge for all the studied NGM@$C_{60}$ systems is higher than that of $C_{60}$, with the largest increase corresponding to NGM=$NH_3$. On the contrary, the trends in electrodonating powers ($\varpi^-$) and in *IE* are quite different. The $\varpi^-$ values of the NGM@$C_{60}$ systems are all higher than that of $C_{60}$, which indicates that their feasibility for donating fractional amounts of charge is lower than that of the empty cage.

It should be noted that for all the studied reactivity indexes the values corresponding to the studied NGM@$C_{60}$ are only

moderately different than those of the empty cage. Therefore, changes in reactivity due to the presence of these guest molecules inside the carbon cage are expected to be only minor.

## Free radical scavenging activity

Free radicals are very reactive chemical species that can be very damaging in both the environment and within living systems. Accordingly, finding viable chemical strategies to deactivate free radicals and, in consequence, avoiding their deleterious effects is currently an active field of investigation. Based on the fullerenes structure two different mechanisms of reaction can be envisaged for their potential free radical scavenging activity. They are: radical adduct formation (RAF) and single electron transfer (SET). In addition, the latter might take place in two different directions from the fullerene to the free radical, or from the free radical to the fullerene. The chemical nature of the reacting free radical will have an important role on determining which of the two directions would prevail.

In this work we have investigated the potential capacity of the studied NGM@$C_{60}$ systems as free radical scavengers, and it has been compared to that of the empty $C_{60}$. This is an attempt to investigate if using this kind of fullerene derivatives might improve this desirable property. In a first stage the RAF reactions of two free radicals with different intrinsic reactivity ($^{\bullet}OOH$ and $^{\bullet}OCH_3$) were investigated in gas phase (vacuum) and also in polar and non-polar solutions. All the studied RAF reactions are predicted to be exothermic (Table 7), while only those involving $^{\bullet}OCH_3$ are predicted to be exergonic. This indicates that the ability of fullerenes to scavenging free radicals via RAF may be determined by the chemical nature of the reacting radical. It was found that the inclusion of the studied NGM inside the $C_{60}$ cage does not significantly increase the thermochemical viability of the radical additions to the C network. The difference, with respect to the empty cage, is below the quantum accuracy (1 kcal mol$^{-1}$) in all the studied cases. On the other hand, the presence of a solvent (regardless its polarity) seems to moderately increase the viability of the RAF reactions compared to those modeled in vacuum. The increment in polarity only leads to a very slight increase in the viability of these reactions.

Since the nature of the reacting free radical has been identified as an important factor in the scavenging activity of chemical compounds [61], and according to the results presented in the previous sections the electronic properties of the fullerenes studied in this work change when $C_{60}$ is hosting NGM, we have studied the SET reactions for a much larger set of free radicals (Table 8). The SET processes were investigated in both directions, i.e., from fullerenes to free radicals (I) and from free radicals to fullerenes (II). The first one is the most common one, since most free radicals are better for accepting than for donating electrons. However, the second one was also included because it has been reported that, at least for the superoxide radical anion ($O_2^{\bullet-}$) when reacting with carotenes [62] it is the relevant SET path. For SET reactions, in direction II, involving radicals R2 and R4 the products corresponding to the radicals after donating one electron decompose. In the case of R2 it expels a $H_2$ molecule, while for R4 the product evolves in such a way that one of the H atoms originally placed in the $CH_2$ group, next to the alkoxyl end, migrates to the O atom. Accordingly, we are not reporting the data for SET II, when these radicals are involved.

**Table 7** Reaction energies for the RAF reactions (kcal mol$^{-1}$), at 298.15 K, in gas phase, and in benzene and water solutions; calculated at the BPW91/6-311+G(d)//BPW91/D95V level of theory

| | $^{\bullet}OCH_3$ | | $^{\bullet}OOH$ | |
|---|---|---|---|---|
| | ΔH | ΔG | ΔH | ΔG |
| Gas | | | | |
| $C_{60}$ | −20.75 | −8.60 | −7.43 | 4.30 |
| $CH_4$@$C_{60}$ | −19.89 | −8.52 | −6.37 | 4.58 |
| $NH_3$@$C_{60}$ | −19.92 | −7.87 | −7.16 | 5.72 |
| $H_2O$@$C_{60}$ | −21.14 | −8.18 | −6.99 | 5.07 |
| HF@$C_{60}$ | −19.80 | −8.34 | −6.14 | 5.47 |
| Benzene | | | | |
| $C_{60}$ | −22.32 | −10.17 | −8.89 | 2.84 |
| $CH_4$@$C_{60}$ | −22.40 | −11.02 | −8.81 | 2.14 |
| $NH_3$@$C_{60}$ | −22.09 | −10.04 | −9.46 | 3.41 |
| $H_2O$@$C_{60}$ | −22.90 | −9.94 | −8.62 | 3.44 |
| HF@$C_{60}$ | −22.42 | −10.96 | −8.75 | 2.86 |
| Water | | | | |
| $C_{60}$ | −23.15 | −11.00 | −10.06 | 1.67 |
| $CH_4$@$C_{60}$ | −22.60 | −11.22 | −9.37 | 1.59 |
| $NH_3$@$C_{60}$ | −22.44 | −10.40 | −9.87 | 3.01 |
| $H_2O$@$C_{60}$ | −23.57 | −10.61 | −9.62 | 2.44 |
| HF@$C_{60}$ | −23.09 | −11.63 | −9.37 | 2.24 |

Contrary to what was found for the RAF mechanism, the polarity of the environment plays a very important role on the thermochemical viability of the SET reactions (Tables 1S to 6S). This is an expected result that goes in line with chemical intuition since polar environments are essential to promote the necessary solvation of the intermediate ionic species yielded by this mechanism. In vacuum, all the studied SET reactions were found to be largely endergonic, with the ΔG values larger than 400 kcal mol$^{-1}$, for both SET directions (Tables 1S and 2S). In benzene solution, the ΔG values are reduced, with respect to gas phase, but all the studied reactions still remain significantly endergonic (Tables 3S and 4S). The only exception is the SET reaction from $O_2^{\bullet-}$ to fullerenes, which is exergonic by more than 30 kcal mol$^{-1}$, in all the studied cases. The same behavior was also found for the SET reactions in direction II when modeled in aqueous solution (Table 6S).

**Table 8** Free radicals modeled for the SET reactions, acronyms, and formulas or structures

| | | |
|---|---|---|
| R1: $^{\bullet}OH$ | R11: $^{\bullet}OOH$ | R21: $^{\bullet}CHCl_2$ |
| R2: $^{\bullet}OCH_3$ | R12: $^{\bullet}OOCH_3$ | R22: $^{\bullet}CCl_3$ |
| R3: $^{\bullet}OCH_2Cl$ | R13: $^{\bullet}OOCH_2Cl$ | R23: $^{\bullet}CH_2CH{=}CH_2$ |
| R4: $^{\bullet}OCH_2CH{=}CH_2$ | R14: $^{\bullet}OOCHCl_2$ | R24: 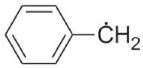 |
| R5: 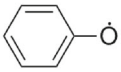 | R15: $^{\bullet}OOCCl_3$ | R25: 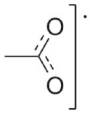 |
| R6: 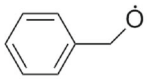 | R16: $^{\bullet}OOCH_2CH{=}CH_2$ | R26: 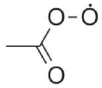 |
| R7: 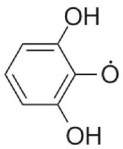 | R17: 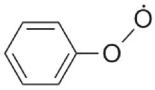 | R27: $^{\bullet}NO_2$ |
| | | R28: $^{\bullet}N_3$ |
| R8: 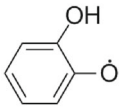 | R18: 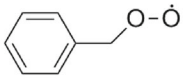 | R29: $O_2^{\bullet-}$ |
| R9: 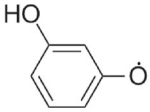 | R19: $^{\bullet}CH_3$ | R30: 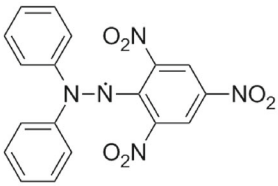 (DPPH) |
| R10: 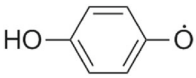 | R20: $^{\bullet}CH_2Cl$ | |

However, in this case the exergonicity is lower than in benzene. The presence of a polar solvent (water in the present study) considerably increases the thermochemical viability of the SET reactions in direction I (Table 5S). Those reactions involving radicals R1, R3, and R25 are exergonic with all the studied fullerenes. In addition the reaction between radical R28 and $C_{60}$ was found to be almost isoergonic, with a ΔG value slightly negative, while for the other studied fullerenes ΔG is positive but very small. The reactions from the studied fullerenes to R15 also present positive but small ΔG values.

For the SET reactions the rate constants were calculated using conventional TST [63–65] as:

$$k = \frac{k_B T}{h} e^{-\left(\Delta G^{\neq}\right)/RT} \tag{12}$$

where $k_B$ and $h$ are the Boltzmann and Planck constants, T is the temperature (K), and $\Delta G^{\neq}$ is the Gibbs free energy of activation, which is calculated using the Marcus theory [66, 67] as:

$$\Delta G^{\neq}_{SET} = \frac{\lambda}{4}\left(1 + \frac{\Delta G^{0}_{SET}}{\lambda}\right)^2 \tag{13}$$

where the $\Delta G^{0}_{SET}$ is the free energy of reaction and $\lambda$ is the nuclear reorganization energy. The later can be calculated using a very simple approximation as:

$$\lambda \approx \Delta E_{SET} - \Delta G^{0}_{SET} \tag{14}$$

where $\Delta E_{SET}$ is the non-adiabatic energy difference between reactants and vertical products. This approach is similar to that previously used by Nelsen and co-workers [68, 69] for a large set of reactions.

The rate constants ($k$) for the SET reactions with values larger than 1 are reported in Tables 9 and 10 for directions I and II, respectively. The reactions with $k \leq 1$ are not reported since they are too slow to have any practical relevance. Some

exceptions are included, when at least one of the *k* values for a particular free radical is>1. The SET reactions from $O_2^{\bullet-}$ to the studied fullerenes were all found to be within or very near to the diffusion controlled regime (Table 9). Accordingly, all the studied fullerenes are proposed to be efficient for scavenging $O_2^{\bullet-}$ via SET. However some differences can be observed. These reactions are predicted to be somehow faster in benzene than in aqueous solution. In addition, our results indicate that while in benzene the reactions of $O_2^{\bullet-}$ with the studied fullerenes are similarly fast, in aqueous solution a distinctive trend arises. Under such conditions the order of reactivity for the studied fullerenes toward $O_2^{\bullet-}$ was found to be HF@$C_{60}$> $C_{60}$>$CH_4$@$C_{60}$>$H_2O$@$C_{60}$>$NH_3$@$C_{60}$.

For the SET reactions in direction I (Table 10) it was found that radicals R1, R3, R15, R25, and R28 are those with the highest rate constants. In fact, they were found to be within, or near to, the diffusion controlled regime. This suggests that the studied fullerenes should be particularly efficient for scavenging these radicals in aqueous solution. In the same environment, the scavenging ability of the studied fullerenes toward radicals R14, R26, and R27 is also expected to be very good. In general, the empty $C_{60}$ was found to react faster than the studied NGM@$C_{60}$. The exceptions correspond to the reactions of $NH_3$@$C_{60}$ and $H_2O$@$C_{60}$ with R1, R3 and R25, which are slightly faster for the endohedral derivatives than for the empty fullerene. In the case of peroxyl radicals the degree of chlorination seems to increase their reactivity toward fullerenes, through SET I. A similar trend should also be expected for other halogenated peroxyl radicals, since their electrophilicity is expected to increase with halogenation.

According to the above discussed results, it is proposed that the main effect of the presence of the studied NGM inside $C_{60}$ on the reactivity of the NGM@$C_{60}$ toward free radicals is related to the increased solubility, rather than to the intrinsic reactivity. This can be important in biological systems where solubility plays an important role on the accessibility of free radical scavengers to different regions. Further increments in reactivity toward free radicals might be attained by more drastic structural modifications, such as functionalizing or doping the C network, which has been proposed to have such effects for carbon nanotubes [70, 71].

**Table 9** Rate constants for the SET reactions ($M^{-1}$ $s^{-1}$) involving electron transfers from free radicals to fullerenes, at 298.15 K, in benzene and aqueous solutions, calculated at the BPW91/6-311+G(d)//BPW91/D95V level of theory

| | $C_{60}$ | $CH_4$@$C_{60}$ | $NH_3$@$C_{60}$ | $H_2O$@$C_{60}$ | HF@$C_{60}$ |
|---|---|---|---|---|---|
| Benzene | | | | | |
| R29 | 1.25E+10 | 1.25E+10 | 1.25E+10 | 1.24E+10 | 1.25E+10 |
| Water | | | | | |
| R29 | 1.27E+09 | 9.23E+08 | 3.67E+08 | 4.92E+08 | 1.51E+09 |

**Table 10** Rate constants for the SET reactions ($M^{-1}$ $s^{-1}$) involving electron transfers from fullerenes to free radicals, at 298.15 K, in aqueous solution, calculated at the BPW91/6-311+G(d)//BPW91/D95V level of theory

| | $C_{60}$ | $CH_4$@$C_{60}$ | $NH_3$@$C_{60}$ | $H_2O$@$C_{60}$ | HF@$C_{60}$ |
|---|---|---|---|---|---|
| R1 | 9.19E+09 | 9.08E+09 | 9.30E+09 | 9.45E+09 | 9.10E+09 |
| R2 | 3.06E+01 | 1.62E-03 | 1.35E-08 | 8.73E-06 | 6.57E-04 |
| R3 | 8.23E+09 | 8.16E+09 | 8.29E+09 | 8.40E+09 | 8.17E+09 |
| R4 | 1.84E+02 | 6.10E-02 | 6.07E-06 | 1.13E-03 | 2.51E-02 |
| R6 | 2.26E+04 | 1.75E+02 | 7.26E-01 | 2.02E+01 | 7.83E+01 |
| R13 | 9.32E+02 | 2.03E+00 | 2.22E-03 | 1.21E-01 | 8.70E-01 |
| R14 | 1.33E+06 | 2.96E+04 | 3.37E+02 | 5.61E+03 | 1.40E+04 |
| R15 | 2.37E+09 | 5.15E+08 | 4.44E+07 | 2.50E+08 | 2.94E+08 |
| R25 | 8.07E+09 | 8.01E+09 | 8.14E+09 | 8.22E+09 | 8.02E+09 |
| R26 | 5.12E+07 | 4.93E+06 | 2.75E+05 | 1.93E+06 | 2.61E+06 |
| R27 | 1.18E+06 | 1.33E+05 | 1.06E+04 | 5.93E+04 | 7.21E+04 |
| R28 | 8.55E+09 | 8.19E+09 | 3.41E+09 | 7.91E+09 | 7.92E+09 |

## Deformed atoms in molecules

To analyze in more detail the changes in the studied systems, after accepting or donating one electron, we have computed the DAM of the corresponding species (Fig. 2). The main finding is that the electron excess, or deficiency, is essentially assumed by the C cage. Thus the role of the guest molecule is almost negligible regarding electron transfers. This explains why the *IE* and *EA* values of all the studied fullerenes are very similar, and also that their reactivity toward free radicals via SET, in both directions, is also alike.

As was previously mentioned for the neutral fullerenes, in the ionic species the zones of density depletion are also aligned with the H atoms of the guest molecule. Thus such kind of deformation on the surfaces of the cages are caused by the molecule inside. However in the cationic species the depletion regions on the cage surfaces increase in size while the inner density remains almost the same as that in the neutral species. For the anions, on the other hand, the depletion regions on the surface decrease in size, then again the size of the concentration region inside the cage remains almost unchanged. Therefore it can be stated that the most significant changes in density distribution, after electron transfers, take place on the conjugated C network.

In addition, the NGM@$C_{60}$ with NGM=HF, $H_2O$, and $NH_3$ show significant density voids on the superficial density. On the other hand, when NGM=$CH_4$, the density on the cage is deformed rather than missing. This can be explained by the higher electronegativity of HF, $H_2O$, and $NH_3$, compared to that of $CH_4$ (Table 6). It seems that if the NGM is electronegative enough, it draws part of the superficial electron density into the cage. This is most noticeably when the whole system has lost one electron (cation, Fig. 2).

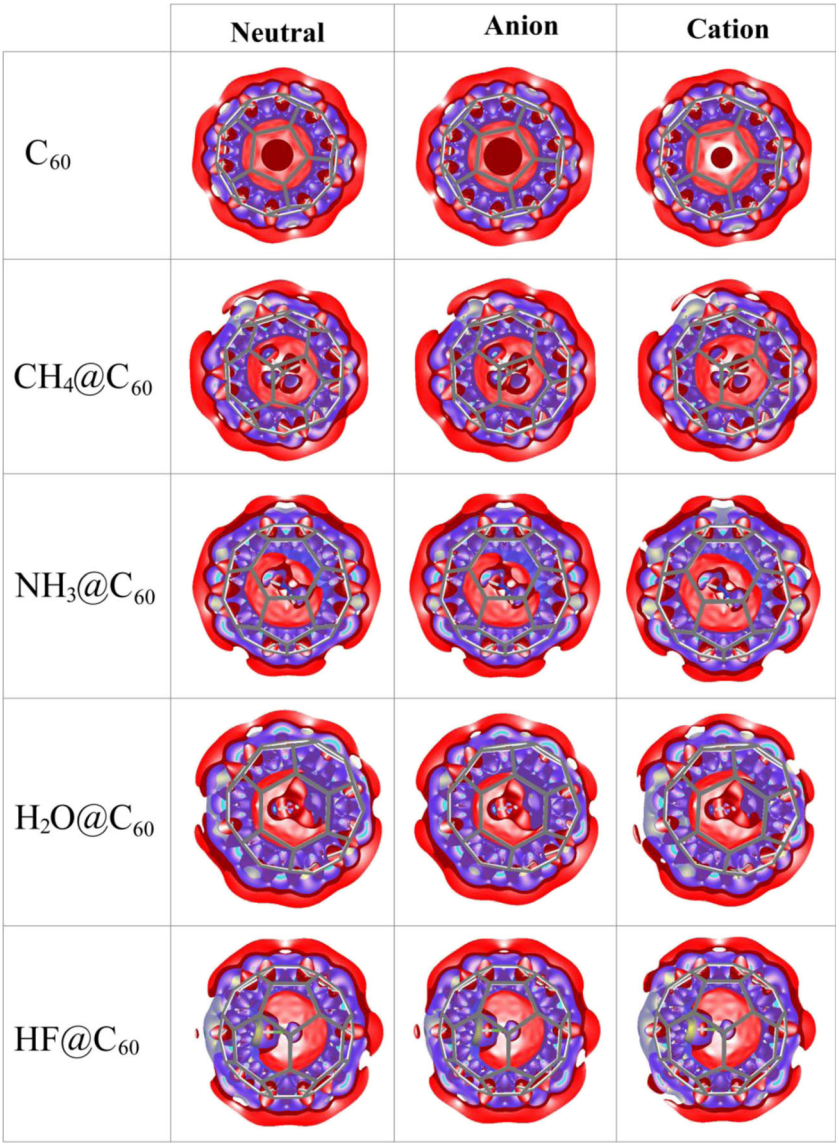


**Fig. 2** Cross-sectional views of the deformed atoms in molecules (DAM) for the neutral, anionic and cationic species of the studied fullerenes. Regions of electron density depletion and concentration are presented in blue and red, respectively. Contour values: ±0.001

## Conclusions

All the studied NGM@$C_{60}$ derivatives (NGM=$CH_4$, $NH_3$, $H_2O$, and HF) are predicted to be stable, with negative binding energies. The influence of the guest molecule on this property was found to be negligible.

Based on dipole moment and polarizabilities analyses it is predicted that the NGM@$C_{60}$ systems should be more soluble in polar solvents than the empty $C_{60}$. This might be relevant for further applications of these systems. The deformations on the surface electron density of the fullerenes allow explaining the polarity and polarizability changes of the NGM@$C_{60}$, compared to those of the empty $C_{60}$.

It was found that the inclusion of the studied NGM inside the $C_{60}$ carbon cage slightly increases the energy of the HOMO. It also lowers (to some extent) the energy of the LUMO, except for NGM=HF. In addition, the HOMO-LUMO gap was found to be moderately smaller for the NGM@$C_{60}$ systems than for the empty cage. All this suggests that the intrinsic reactivity of studied NGM@$C_{60}$ is higher than that of $C_{60}$ but only to a modest extent. The calculated global reactivity indexes support this trend.

The studied fullerenes were found to be able of efficiently scavenging alkoxyl radicals through the radical adduct formation mechanism. It was also found that the scavenging ability of the studied systems through SET strongly depends on the chemical nature of the reacting free radical. In addition this activity is increased by the polarity of the environment when it takes place from fullerenes to free radicals. The presence of the studied NGM inside the $C_{60}$ cage influence only moderately the reactivity of $C_{60}$ toward free radicals.

The studied fullerenes are expected to be efficient deactivating the superoxide radical anion by SET from the radical to the fullerenes. Accordingly they are expected to

prevent the formation of reactive oxygen species that are yielded from $O_2^{\bullet-}$, such as the hydroxyl radical.

When the systems gain or lose one electron, the excess or deficiency on electron density is essentially located on the C cage. Thus the role of the guest molecule is almost negligible regarding electron transfers.

The NGM were found to cause deformations of the cage electron density. The extension of such deformations is directly related to the electron withdrawing capacity of the NGM, while their location depends on the orientation of the H atoms in the NGM.

**Acknowledgments** The authors gratefully acknowledge Prof. Rafael López, at Universidad Autónoma de Madrid for his valuable comments. This work was partially supported by the projects SEP-CONACyT 167491. J.R.L.-C. acknowledges the economic support of the Program of Postdoctoral Scholarships from DGAPA (UNAM). L.O. thanks Project LIQUORGAS-S2009/PPQ-1545, Comunidad de Madrid, for financial support. We thank the Laboratorio de Visualización y Cómputo Paralelo at Universidad Autónoma Metropolitana-Iztapalapa for the access to computing facilities.

## References

1. Saunders M, Jiménez-Vázquez HA, Cross RJ, Poreda RJ (1993) Stable compounds of helium and neon: He@$C_{60}$ and Ne@$C_{60}$. Science 259:1428–1430
2. Saunders M, Cross RJ, Jiménez-Vázquez HA, Shimshi R, Khong A (1996) Noble gas atoms inside fullerenes. Science 271:1693–1697
3. Pietzak B, Waiblinger M, Almeida MT, Weidinger A, Höhne M, Dietel E, Hirsch A (1997) Buckminsterfullerene $C_{60}$: a chemical faraday cage for atomic nitrogen. Chem Phys Lett 279:259–263
4. Shabtai E, Weitz A, Haddon RC, Hoffman RE, Rabinovitz M, Khong A, Cross RJ, Saunders M, Cheng PC, Scott LT (1998) $^3$He NMR of He@$C_{60}{}^{6-}$ and He@$C_{70}{}^{6-}$. New records for the most shielded and the most deshielded $^3$He inside a fullerene. J Am Chem Soc 120: 6389–6393
5. Nishibori E, Takata M, Sakata M, Tanaka H, Hasegawa M, Shinohara H (2000) Giant motion of La atom inside $C_{82}$ cage. Chem Phys Lett 330:497–502
6. Peres T, Cao B, Cui W, Khong A, Cross RJ, Saunders M, Lifshitz C (2001) Some new diatomic molecule containing endohedral fullerenes. Int J Mass Spectrom 210:241–247
7. Murata Y, Murata M, Komatsu K (2003) 100 % encapsulation of a hydrogen molecule into an open-cage fullerene derivative and gas-phase generation of $H_2$@$C_{60}$. J Am Chem Soc 125:7152–7153
8. Shimotani H, Ito T, Iwasa Y, Taninaka A, Shinohara H, Nishibori E, Takata M, Sakata M (2004) Quantum chemical study on the configurations of encapsulated metal ions and the molecular vibration modes in endohedral dimetallofullerene $La_2$@$C_{80}$. J Am Chem Soc 126:364–369
9. Murata M, Murata Y, Komatsu K (2006) Synthesis and properties of endohedral $C_{60}$ encapsulating molecular hydrogen. J Am Chem Soc 128:8024–8033
10. Cimpoesu F, Ito S, Shimotani H, Takagi H, Dragoe N (2011) Vibrational properties of noble gas endohedral fullerenes. Phys Chem Chem Phys 13:9609–9615
11. Kurotobi K, Murata Y (2011) A single molecule of water encapsulated in fullerene $C_{60}$. Science 333:613–616
12. Sabirov DS (2013) From endohedral complexes to endohedral fullerene covalent derivatives: a density functional theory prognosis of chemical transformation of water endofullerene $H_2O$@$C_{60}$ upon its compression. J Phys Chem C 117:1178–1182
13. Murata M, Murata Y, Komatsu K (2008) Surgery of fullerenes. Chem Commun 46:6083–6094
14. Whitener KE, Frunzi M, Iwamatsu S, Murata S, Cross RJ, Saunders M (2008) Putting ammonia into a chemically opened fullerene. J Am Chem Soc 130:13996–13999
15. Stanisky CM, Cross RJ, Saunders M (2009) Putting atoms and molecules into chemically opened fullerenes. J Am Chem Soc 131: 3392–3395
16. Balch AL (2011) $H_2O$ in a desert of carbon atoms. Science 333:531–532
17. Beduz C, Carravetta M, Chen JYC, Concistrè M, Denning M, Frunzi M, Horsewill AJ, Johannessen OG, Lawler R, Lei X, Levitt MH, Li Y, Mamone S, Murata Y, Nagel U, Nishida T, Ollivier J, Rols S, Rõõm T, Sarkar R, Turro NJ, Yang Y (2012) Quantum rotation of *ortho* and *para*-water encapsulated in a fullerene cage. Proc Natl Acad Sci 109:12894–12898
18. Li Y, Chen JYC, Lei X, Lawler RG, Murata Y, Komatsu K, Turro NJ (2012) Comparison of nuclear spin relaxation of $H_2O$@$C_{60}$ and $H_2$@$C_{60}$ and their nitroxide derivatives. J Phys Chem Lett 3:1165–1168
19. Zhang R, Murata M, Wakamiya A, Murata Y (2013) Synthesis and X-ray structure of endohedral fullerene C60 dimer encapsulating a water molecule in each C60 cage. Chem Lett 42:879–881
20. Ramachandran CN, Sathyamurthy N (2005) Water clusters in a confined nonpolar environment. Chem Phys Lett 410:348–351
21. Yagi K, Watanabe D (2009) Infrared spectra of water molecule encapsulated inside fullerene studied by instantaneous vibrational analysis. Int J Quantum Chem 109:2080–2090
22. Bucher D (2012) Orientational relaxation of water trapped inside $C_{60}$ fullerenes. Chem Phys Lett 534:38–42
23. Hernández-Rojas J, Monteseguro V, Bretón J, Gomez-Llorente JM (2012) Water clusters confined in icosahedral fullerene cavities. Chem Phys 399:240–244
24. Xu B, Chen X (2013) Electrical-driven transport of endohedral fullerene encapsulating a single water molecule. Phys Rev Lett 110: 156103, 5 pages
25. Rehaman A, Gagliardi L, Pyykkö P (2007) Pocket and antipocket conformations for the $CH_4$@$C_{84}$ endohedral fullerene. Int J Quantum Chem 107:1162–1169
26. Ren XY, Jiang CY, Wang J, Liu ZY (2008) Endohedral complex of fullerene $C_{60}$ with tetrahedrane, $C_4H_4$@$C_{60}$. J Mol Graph Model 27: 558–562
27. Ren XY, Jiang CY (2012) Density functional studies on the endohedral complex of fullerene $C_{70}$ with tetrahedrane ($C_4H_4$): $C_4H_4$@$C_{70}$. J Mol Model 18:3213–3217
28. Wang GW, Wu P, Tian ZG (2009) Endohedral $^1$H NMR chemical shifts of $H_2$-, $H_2O$- and $NH_3$-encapsulated fullerene compounds: accurate calculation and prediction. Eur J Org Chem 2009:1032–1041
29. Peng S, Li XJ, Zhang DX, Zhang Y (2009) A computational study of the endohedral fullerene $GeH_4$@$C_{60}$. Struct Chem 20:789–794
30. Medrek M, Pluciński F, Mazurek AP (2013) Endohedral complexes of fullerene $C_{60}$ with small convalent molecules ($H_2O$, $NH_3$, $H_2$, $2H_2$, $3H_2$, $4H_2$, $O_2$, $O_3$) in the context of potential drug transporter system. Acta Pol Pharm 70:659–665
31. Krusic PJ, Wasserman E, Keizer PN, Morton JR, Preston KF (1991) Radical reactions of $C_{60}$. Science 254:1183–1185
32. McEwen CN, McKay RG, Larsen BS (1992) $C_{60}$ as a radical sponge. J Am Chem Soc 114:4412–4414
33. Gan L, Huang S, Zhang X, Zhang A, Cheng B, Cheng H, Li X, Shang G (2002) Fullerenes as a tert-butylperoxy radical trap, metal

catalyzed reaction of tert-butyl hydroperoxide with fullerenes, and formation of the first fullerene mixed peroxides $C_{60}(O)(OO^tBu)_4$ and $C_{70}(OO^tBu)_{10}$. J Am Chem Soc 124:13384–13385
34. Morton JR, Preston KF, Krusic PJ, Hill SA, Wasserman E (1992) ESR studies of the reaction of alkyl radicals with fullerene (C60). J Phys Chem 96:3576–3578
35. Borghi R, Lunazzi L, Placucci G, Krusic PJ, Dixon DA, Matsuzawa N, Ata M (1996) Addition of aryl and fluoroalkyl radicals to fullerene $C_{70}$: ESR detection of five regioisomeric adducts and density functional calculations. J Am Chem Soc 118:7608–7617
36. Frisch MJ, Trucks GW, Schlegel HB, Scuseria GE, Robb MA, Cheeseman JR, Scalmani G, Barone V, Mennucci B, Petersson GA, Nakatsuji H, Caricato M, Li X, Hratchian HP, Izmaylov AF, Bloino J, Zheng G, Sonnenberg JL, Hada M, Ehara M, Toyota K, Fukuda R, Hasegawa J, Ishida M, Nakajima T, Honda Y, Kitao O, Nakai H, Vreven T, Montgomery JA, Peralta JE, Ogliaro F, Bearpark M, Heyd JJ, Brothers E, Kudin KN, Staroverov VN, Kobayashi R, Normand J, Raghavachari K, Rendell A, Burant JC, Iyengar SS, Tomasi J, Cossi M, Rega N, Millam NJ, Klene M, Knox JE, Cross JB, Bakken V, Adamo C, Jaramillo J, Gomperts R, Stratmann RE, Yazyev O, Austin AJ, Cammi R, Pomelli C, Ochterski JW, Martin RL, Morokuma K, Zakrzewski VG, Voth GA, Salvador P, Dannenberg JJ, Dapprich S, Daniels AD, Farkas O, Foresman JB, Ortiz JV, Cioslowski J, Fox DJ (2009) Gaussian 09, Revision A.08. Gaussian, Inc, Wallingford
37. Dunning TH, Hay PJ (1976) Modern theoretical chemistry. Schaefer HF III (ed) vol. 3, Plenum, New York, pp 1–28
38. Becke AD (1988) Density-functional exchange-energy approximation with correct asymptotic behavior. Phys Rev A 38: 3098–3100
39. Burke K, Perdew JP, Wang Y (1998) In: Electronic density functional theory: recent progress and new directions. Dobson JF, Vignale G, and Das MP (eds) Plenum, New York,pp 81–111
40. Perdew JP (1991) In: Electronic structure of solids'91. Ziesche P and Eschrig H (eds). Akademie, Berlin, pp 11–20
41. Perdew JP, Chevary JA, Vosko SH, Jackson KA, Pederson MR, Singh DJ, Fiolhais C (1992) Atoms, molecules, solids, and surfaces: applications of the generalized gradient approximation for exchange and correlation. Phys Rev B 46:6671–6687
42. Perdew JP, Burke K, Wang Y (1996) Generalized gradient approximation for the exchange-correlation hole of a many-electron system. Phys Rev B 54:16533–16539
43. Marenich AV, Cramer CJ, Truhlar DG (2009) Universal solvation model based on solute electron density and on a continuum model of the solvent defined by the bulk dielectric constant and atomic surface tensions. J Phys Chem B 113:6378–6396
44. López R, Fernández-Rico J, Ramírez G, Ema I, Zorrilla D (2009) DAMQT: a package for the analysis of electron density in molecules. Comput Phys Commun 180:1654–1660
45. Lichtenberger DL, Nebesny KW, Ray CD, Huffman DR, Lamb LD (1991) Valence and core photoelectron spectroscopy of $C_{60}$, buckminsterfullerene. Chem Phys Lett 176:203–208
46. Palpant B, Negishi Y, Sanekata M, Miyajima K, Nagao S, Judai K, Rayner DM, Simard B, Hackett PA, Nakajima A, Kaya K (2001) Electronic and geometric properties of exohedral sodium- and gold-fullerenes. J Chem Phys 114:8459–8466
47. Yao X, Ruskell TG, Workman RK, Sarid D, Chen D (1996) Scanning tunneling microscopy and spectroscopy of individual C60 molecules on Si(100)-2×1 surfaces. Surf Sci Lett 366:L743–L749
48. Compagnon I, Antoine R, Broyer M, Dugourd P, Lermé J, Rayane D (2001) Electric polarizability of isolated $C_{70}$ molecules. Phys Rev A 64:025201, 4 pages
49. Fukui K, Yonezawa T, Shingu H (1952) A molecular orbital theory of reactivity in aromatic hydrocarbons. J Chem Phys 20:722–725
50. Fukui K (1971) Recognition of stereochemical paths by orbital interaction. Acc Chem Res 4:57–64
51. Manolopoulos DE, May JC, Down SE (1991) Theoretical studies of the fullerenes: $C_{34}$ to $C_{70}$. Chem Phys Lett 181:105–111
52. Liu X, Schmalz TG, Klein DJ (1992) Favorable structures for higher fullerenes. Chem Phys Lett 188:550–554
53. Diener MD, Alford JM (1998) Isolation and properties of small-bandgap fullerenes. Nature 393:668–671
54. Parr RG, Pearson RG (1983) Absolute hardness: companion parameter to absolute electronegativity. J Am Chem Soc 105:7512–7516
55. Parr RG, Donnelly RA, Levy M, Palke WE (1978) Electronegativity: the density functional viewpoint. J Chem Phys 68:3801–3807
56. Parr RG, Yang W (1989) Density-functional theory of atoms and molecules. Oxford University Press, New York
57. Chattaraj PK, Maiti B, Sarkar U (2003) Philicity: a unified treatment of chemical reactivity and selectivity. J Phys Chem A 107:4973–4975
58. Parr RG, Szentpaly L, Liu S (1999) Electrophilicity index. J Am Chem Soc 121:1922–1924
59. Gazquez JL, Cedillo A, Vela A (2007) Electrodonating and electroaccepting powers. J Phys Chem A 111:1966–1970
60. Gázquez JL (2008) Perspectives on the density functional theory of chemical reactivity. J Mex Chem Soc 52:3–10
61. Galano A, Álvarez-Diduk R, Ramírez-Silva MT, Alarcón-Ángeles G, Rojas-Hernández A (2009) Role of the reacting free radicals on the antioxidant mechanism of curcumin. Chem Phys 363:13–23
62. Galano A, Vargas R, Martinez A (2010) Carotenoids can act as antioxidants by oxidizing the superoxide radical anion. Phys Chem Chem Phys 12:193–200
63. Eyring H (1935) The activated complex in chemical reactions. J Chem Phys 3:107–115
64. Evans MG, Polanyi M (1935) Some applications of the transition state method to the calculation of reaction velocities, especially in solution. Trans Faraday Soc 31:875–894
65. Truhlar DG, Hase WL, Hynes JT (1983) Current status of transition-state theory. J Phys Chem 87:2664–2682
66. Marcus RA (1965) Chemical and electrochemical electron-transfer theory. Annu Rev Phys Chem 15:155–196
67. Marcus RA (1993) Electron transfer reactions in chemistry. Theory and experiment. Rev Mod Phys 65:599–610
68. Nelsen SF, Blackstock SC, Kim Y (1987) Estimation of inner shell Marcus terms for amino nitrogen compound by molecular orbital calculations. J Am Chem Soc 109:677–682
69. Nelsen SF, Weaver MN, Luo Y, Pladziewicz JR, Ausman LK, Jentzsch TL, O'Konek JJ (2006) Estimation of electronic coupling for intermolecular electron transfer from cross-reaction data. J Phys Chem A 110:11665–11676
70. Francisco-Marquez M, Galano A, Martinez A (2010) On the free radical scavenging capability of carboxylated single-walled carbon nanotubes. J Phys Chem C 114:6363–6370
71. Martínez A, Francisco-Marquez M, Galano A (2010) Effect of different functional groups on the free radical scavenging capability of single-walled carbon nanotubes. J Phys Chem C 114:14734–14739